

MECHANISM OF THE 1983 COALINGA EARTHQUAKE  
DETERMINED FROM LONG-PERIOD SURFACE WAVES

by

Hiroo Kanamori<sup>1</sup>

ABSTRACT

The mechanism of the May 2, 1983, Coalinga, California earthquake determined from long-period surface waves and first-motion data is given by dip angle =  $65^{\circ}$ , strike =  $N58^{\circ}W$ , rake =  $70^{\circ}$ , seismic moment =  $5.4 \times 10^{25}$  dyne-cm ( $M_w = 6.4$ ), and the source process time  $\approx 20$  sec. The local magnitude,  $M_L$ , is estimated to be  $6.43 \pm 0.27$ . On the  $M_L$  vs.  $M_w$  diagram, the Coalinga earthquake falls on the average trend for California earthquakes.

<sup>1</sup>Seismological Laboratory, California Institute of Technology, Pasadena, CA 91125

## INTRODUCTION

We report the source parameters of the 1983 Coalinga, California, earthquake (May 2, 23<sup>h</sup> 42<sup>m</sup> 37.8<sup>s</sup>, 36°13.99'N, 120°17.59'W, 10.5 km, Eaton, 1983) determined from long-period (256 sec) surface waves recorded by the digital stations of the IDA (International Deployment of Accelerometers) network and the Global Digital Seismographic Network (GDSN).

The mechanism solution obtained from long-period surface waves represents the overall fault geometry, and provides a reliable estimate of the seismic moment.

## ANALYSIS

The stations and the phases used are listed in Table 1. In total, 40 Rayleigh- and Love-wave phases from 19 stations are used. Using the method described by Kanamori and Given (1981), we inverted the spectral data of these surface waves at a period of 256 sec to determine the seismic moment tensor and the fault model.

Since the source depth reported by Eaton (1983) is 10.5 km, we used a point source at a depth of 9.75 km, the depth closest to 10.5 km where the excitation functions are tabulated in Kanamori and Given (1981). As is discussed by Kanamori and Given (1981), the two elements of the moment tensor,  $M_{zx}$  and  $M_{zy}$  are indeterminate for shallow events. Hence, we first set  $M_{zx} = M_{zy} = 0$  which is equivalent to restricting the solution either to a 45° dip-slip or a vertical strike-slip fault. Despite this restriction, the solutions obtained with these constraints provide useful gross estimates of fault geometry and seismic moment.

Empirical relations (Furumoto, 1979, Furumoto and Nakanishi, 1983; Dziewonski and Woodhouse, 1983) suggest a source process time,  $\tau$ , of about 10 sec for earthquakes with  $M_s \approx 6.5$ . We inverted the Rayleigh-wave data, varying  $\tau$  from 0 to 50 sec, and found that  $\tau = 20$  sec provides a best fit. Since the regional variation of Love-wave phase velocity is very large even at a period of 256 sec, we did not include Love waves for the determination of  $\tau$ . Although this value is somewhat larger than that empirically expected, the difference is probably insignificant. Nakanishi and Kanamori (1983) obtained a standard deviation of 17 sec for the measurement of the source process time from a global data set.

Using  $\tau = 20$  sec, we inverted the Rayleigh- and Love-wave spectral data together. The results are shown in Table 2, Figure 1 and Figure 2. The moment tensor can be decomposed into the major and minor double couples. The mechanism of the major double couple (constrained to be either a 45° dip-slip or a vertical strike slip) is a 45° thrust fault

with a strike of  $N36^{\circ}W$ . The seismic moment is  $4.4 \times 10^{25}$  dyne-cm. The moment of the minor double couple is only 8.9% of that of the major double couple, and is considered insignificant.

If we assume that the geometry of the source did not change during faulting, we can combine P-wave first-motion data with the surface-wave data to determine further details of the source geometry (Kanamori and Given, 1981). First-motion data were obtained from selected WWSSN (Worldwide Standardized Seismographic Network) and Canadian Network stations (Hartzell and Heaton, 1983, this volume), and RSTN (Regional Seismic Test Network) stations. These data are listed in Table 3. We computed the take-off angles using the Jeffreys-Bullen travel time curves with the velocity at the source of 6.5 km/sec. Stations ALE, VAL, WES and RSCP show a very small upward first-motion followed by a large downward motion, suggesting that these stations are located very close to the node of the P-wave radiation pattern. These stations together with other stations determine one of the nodal planes very well as shown by Figure 2. The strike of this plane is  $N58^{\circ}W$  which agrees very well with that determined by Eaton (1983) from local data ( $N53^{\circ}W$ ). The teleseismic first-motion data provide no constraint on the other nodal plane.

We then fixed the steep nodal plane and inverted the Rayleigh- and Love-wave data to determine the rake  $\lambda$  on this plane and the seismic moment. The result is shown in Table 4 and Figure 2. The RMS (root-mean-square) value of the difference between the observed and computed spectra is 0.0242 cm-sec, which is only slightly larger than that for the constrained moment tensor solution, 0.0239 cm-sec, indicating that this mechanism is a good fit to the surface-wave data. The rake on the steeply dipping plane is  $70^{\circ}$  which makes the strike of the second nodal plane almost north-south. The seismic moment for this solution is  $5.4 \times 10^{25}$  dyne-cm. Changing the depth from 9.75 to 16 km only increases the moment by 8%. This geometry is very similar to that determined by Hartzell and Heaton (1983, in this volume) from body-wave data and to that determined by inversion of GDSN waveform data (A. Dziewonski, personal communication, July 20, 1983).

Considering the relatively short source process time, the assumption that the geometry of the source for body waves is the same as that for surface waves is reasonable. Hence, we prefer this solution as the mechanism of the 1983 Coalinga earthquake.

#### CONCLUSION

The mechanism of the 1983 Coalinga, California, earthquake determined from long-period surface waves and first-motion data is given in Table 3 and Figure 2. The seismic moment is  $5.4 \times 10^{25}$  dyne-cm and  $M_w = 6.4$ . The source process time is about 20 sec; no evidence for anomalously

long source process is found.

The strike of the aftershock area reported by Eaton (1983) is about N38°W and is more parallel to the steeply dipping nodal plane than to the low-angle nodal plane of our solution, suggesting that the steep plane is the fault plane.

The local magnitudes of the Coalinga earthquake determined from six Wood-Anderson records obtained from the Southern California Network are listed in Table 5. From these data, we obtain  $M_L = 6.20 \pm 0.11$ . The local magnitude determined from the network of the University of California, Berkeley, is  $6.70 \pm 0.16$  (five observations) (B. A. Bolt, written communication, August, 1983, also this volume). The average of these two values weighted by the number of records used for each determination is  $M_L = 6.43 \pm 0.27$ . Figure 3 compares the Coalinga earthquake with other earthquakes in California (the 1976 Guatemala earthquake is included for comparison) on the  $M_L$  vs.  $M_W$  diagram which has been used to compare the high-frequency characteristics of earthquakes (Kanamori and Regan, 1982). The Coalinga earthquake falls on the average trend for California earthquakes.

#### ACKNOWLEDGMENTS

I thank Jon Berger and Jeffrey Given for their help in retrieving the RSTN data, and Bruce Bolt for providing me with the  $M_L$  data from the Berkeley network. I also thank Tom Heaton and Stephen Hartzell for useful information on their body-wave solution. The IDA and GDSN data were provided by the University of California, San Diego, and the U. S. Geological Survey respectively. This research was partially supported by U. S. Geological Survey contract No. 14-08-0001-21210. Contribution No. 3958, Division of Geological and Planetary Sciences, California Institute of Technology, Pasadena, California 91125.

#### REFERENCES

- Dziewonski, A. M., and Woodhouse, J. H., 1983, An experiment in systematic study of global seismicity: Centroid-moment tensor solutions for 201 moderate and large earthquakes of 1981, *J. Geophys. Res.*, v. 88, p. 3247-3271.
- Eaton, J. P., 1983, Seismic setting, location and focal mechanism of the May 2, 1983, Coalinga earthquake, U. S. Geological Survey, Open-File Report 83-511, p. 20-26.
- Furumoto, M., 1979, Initial phase analysis of R-waves from great earthquakes, *J. Geophys. Res.*, v. 84, p. 6867-6874.
- Furumoto, M., and Nakanishi, I., 1983, Source times and scaling relations of large earthquakes, *J. Geophys. Res.*, v. 88, p. 2191-2198.
- Kanamori, H., and Given, J. W., 1981, Use of long-period surface waves for rapid determination of earthquake-source parameters, *Phys. Earth and Planet. Int.*, v. 27, p. 8-31.

Kanamori, H., and Regan, J., 1982, Long-period surface waves, the Imperial Valley, California, earthquake of October 15, 1979, U. S. Geological Survey Professional Paper 1254, p. 55-58.

Nakanishi, I., and Kanamori, H., 1983, Source mechanisms of twenty-six large shallow earthquakes ( $M_s > 6.5$ ) during 1980 from P-wave first motion and long-period Rayleigh wave data, submitted to Seismol. Soc. Amer. Bull.

Table 1

| Station | $\Delta$<br>(deg.) | $\phi$<br>(deg.) | Phases          |
|---------|--------------------|------------------|-----------------|
| SJG     | 51.0               | 95.7             | $R_2, R_3$      |
| KIP     | 36.1               | 256.3            | $R_2, R_3$      |
| TWO     | 117.8              | 245.7            | $R_1, R_2$      |
| CMO     | 32.9               | 338.8            | $R_2, R_3$      |
| KMY     | 106.6              | 319.9            | $R_1, R_2$      |
| ALE     | 50.0               | 8.3              | $R_2, R_3$      |
| RAR     | 68.4               | 219.8            | $R_2$           |
| ERM     | 71.0               | 308.6            | $R_2$           |
| ESK     | 74.0               | 31.9             | $R_2, R_3$      |
| HAL     | 43.3               | 60.6             | $R_2, R_3$      |
| ANTO    | 100.2              | 20.7             | $R_1, R_2, G_1$ |
| GUMO    | 86.0               | 283.9            | $R_1, R_2, G_1$ |
| NWAO    | 133.2              | 256.8            | $R_1, R_2, G_1$ |
| TATO    | 95.7               | 306.7            | $R_1, R_2, G_1$ |
| SNZO    | 97.5               | 223.7            | $R_1, R_2$      |
| CTAO    | 104.4              | 255.7            | $R_1, R_2, G_1$ |
| ZOBO    | 71.8               | 126.9            | $R_2$           |
| KONO    | 75.8               | 23.6             | $R_1, R_2, G_1$ |
| MAJO    | 77.3               | 306.1            | $G_1$           |

Note:  $\Delta$  is the distance and  $\phi$  is the azimuth measured clockwise from the north.

Table 2

## Constrained Moment Tensor

( $M_{zx} = M_{zy} = 0$ ,  $d = 9.75$  km,  $\tau = 20$  sec)

| $M_{xy}$        | $M_{yy} - M_{xx}$ | $M_{yy} + M_{xx}$ |
|-----------------|-------------------|-------------------|
| $2.3 \pm 0.3^*$ | $-1.5 \pm 0.6^*$  | $-4.0 \pm 0.3^*$  |

## Major Double Couple

| Moment | dip | rake | Strike | dip | rake | strike | RMS      |
|--------|-----|------|--------|-----|------|--------|----------|
| 4.4*   | 45° | 90°  | 144°   | 45° | 90°  | -36°   | 0.0239** |

Minor Double Couple - 8.9% of the Major Double Couple

\* unit  $10^{25}$ dyne-cm

\*\* unit cm-sec

Table 3

## First-Motion Data

| Station | $\Delta$ (deg.) | $\phi$ (deg.) | $i_h$ (deg.) | First Motion |
|---------|-----------------|---------------|--------------|--------------|
| AFI     | 69.6            | 234           | 20.1         | U            |
| AKU     | 62.3            | 27            | 22.6         | U            |
| ALE     | 50.2            | 8             | 27.2         | Nodal Up     |
| BOG     | 52.8            | 115           | 26.0         | U            |
| COP     | 80.0            | 24            | 19.3         | U            |
| ESK     | 74.2            | 31            | 19.2         | U            |
| KON     | 75.9            | 23            | 19.2         | U            |
| LPA     | 91.5            | 133           | 16.0         | U            |
| LPS     | 35.4            | 120           | 30.0         | U            |
| MAT     | 77.4            | 306           | 19.7         | U            |
| SHK     | 82.2            | 307           | 18.5         | U            |
| VAL     | 73.1            | 37            | 19.2         | Nodal Up     |
| WES     | 38.0            | 65            | 30.7         | Nodal Up     |
| FFC     | 22.4            | 28            | 33.8         | D            |
| PHC     | 15.4            | 342           | 49.7         | D            |
| RSCP    | 28.0            | 80            | 33.5         | Nodal Up     |
| RSNY    | 35.4            | 62            | 30.1         | D            |
| RSSD    | 14.7            | 52            | 49.8         | D            |
| RSON    | 24.0            | 44            | 33.3         | D            |

Note:  $\Delta$  is the distance,  $\phi$  is the azimuth measured clockwise from the north, and  $i_h$  is the take-off angle.

Table 4

## Fault Inversion

(Depth 9.75 km, Source Process Time = 20 sec)

|                    |  |
|--------------------|--|
| Seismic Moment     | (5.4 + 0.3) x 10 <sup>25</sup> dyne-cm |
| First Nodal Plane  |  |
| Dip                | 65° (Constrained)                      |
| Strike             | 70 ± 3°                                |
| Strike             | -58° (Constrained)                     |
| Second Nodal Plane |  |
| Dip                | 32°                                    |
| Strike             | 126°                                   |
| Strike             | 163°                                   |
| P axis             |  |
| Azimuth            | 47°                                    |
| Plunge             | 18°                                    |
| T axis             |  |
| Azimuth            | 178°                                   |
| Plunge             | 64°                                    |
| RMS                | 0.0242 cm-sec                          |

Table 5

## Wood-Anderson Amplitude Data from Southern California Network

| Station | Comp. | $\Delta$<br>(km) | Azimuth<br>(Deg.) | Amp.<br>mm | $M_L^*$ |
|---------|-------|------------------|-------------------|------------|---------|
| RVR     | NS    | 364              | 132               | 53.0       | 6.12    |
| RVR     | EW    | 364              | 132               | 70.0       | 6.25    |
| PLM     | NS    | 448              | 135               | 35.2       | 6.15    |
| PLM     | EW    | 448              | 135               | 64.8       | 6.41    |
| PAS     | NS    | 301              | 140               | 99.6       | 6.11    |
| PAS     | EW    | 301              | 140               | 116.0      | 6.17    |

Av. 6.20 ± 0.11

\* Station correction, 0.1 unit is added for RVR and PAS.

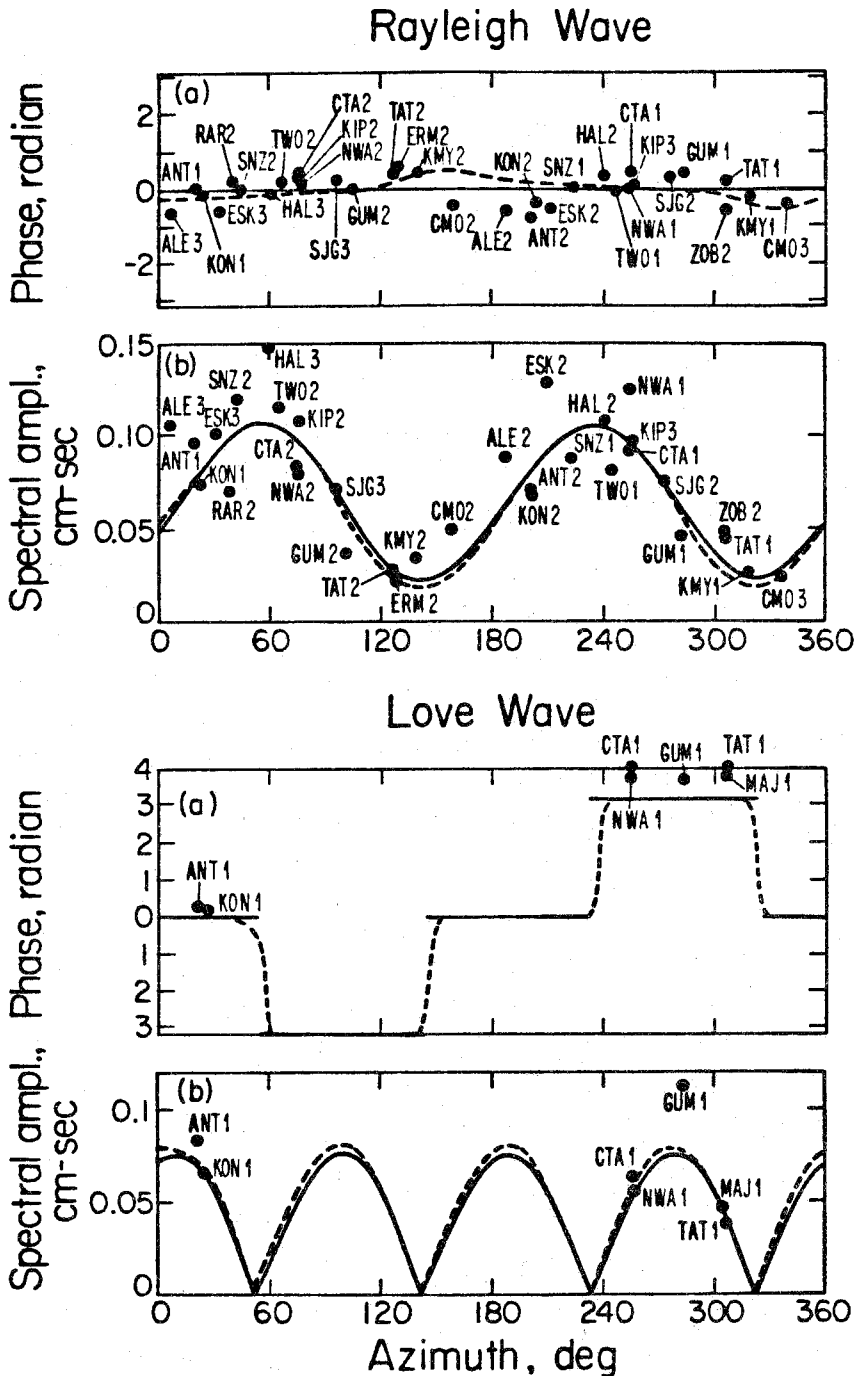


Figure 1. Phase (a) and amplitude (b) spectra of Rayleigh and Love waves at a period of 256 sec. Each data point represents the source spectrum at each station. The three-letter station code and phase number are attached to each data point. Solid and dashed curves are computed for the constrained moment tensor (Table 2) and the fault model (Table 4) respectively.

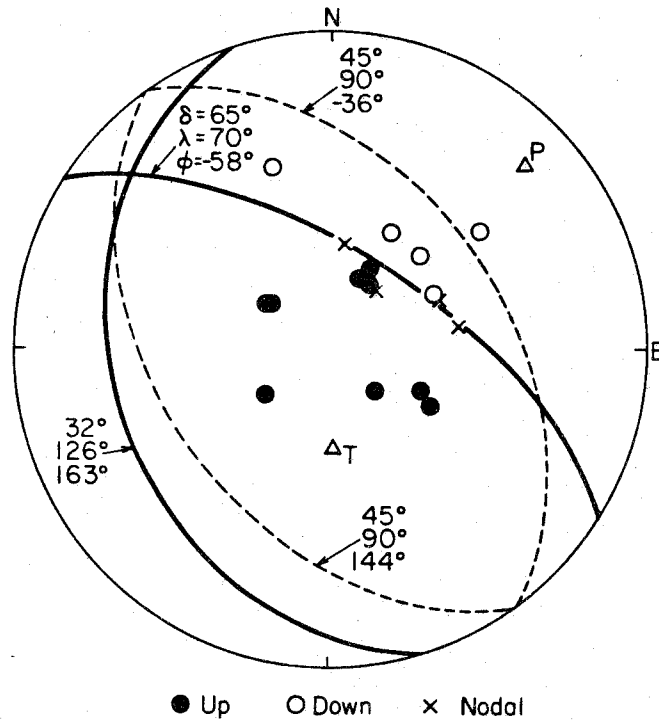


Figure 2. First-motion data and the nodal lines for the major double couple of the moment tensor solution (Table 2, dashed curve) and the fault model (Table 4, solid curve).

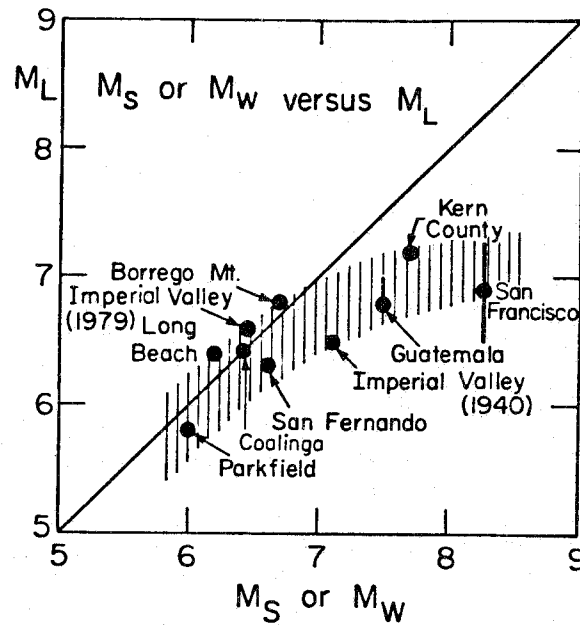


Figure 3. The relation between local magnitude,  $M_L$ , and moment magnitude,  $M_W$ , (or surface-wave magnified  $M_S$ ) for California earthquakes and the 1976 Guatemala earthquake. Diagonal line represents  $M_L = M_W$  (or  $M_S$ ), band of vertical lines defines range of  $M_L$  at a given  $M_W$  (or  $M_S$ ) for California earthquakes.